TEKNOLOGI DAN KEJURUAN, VOL. 38, NO. 1, FEBRUARI 2015: 89-104

# NUMERICAL SIMULATION OF FRAME STRUCTURE ON SHALLOW FOUNDATION WITH EXPANDED POLYSTYRENE (EPS)

**Indra Waluyohadi**
**Huei-Tsyr Chen**
**Achfas Zacoeb**

**Abstract:** For the past 30 years, applications of expanded polystyrene (EPS) geofoam have been proposed. Several studies have examined the behavior of geofoam and produced beneficial results in the evolution of its application. One of application of expanded polystyrene can be used laid under the grade beam or slab. Meanwhile some of existing structure were suported by shallow foundation. Thus when EPS applied beneath shallow foundation to be alternative design, EPS supposed reduce the seismic response of structure. The purpose of this study is to investigate the seismic response of structure numerically due to application of EPS applied beneath the shallow foundation. In this study, the D7S2 finite element program was adopted to investigate the seismic response of structure due to apllication of EPS applied beneath the shallow foundation subjected to the earthquake motion. Verification and validation of the program was conducted by comparing the results to the shaking table test results. A series of parametric study is conducted including the interface element and the variations of size of EPS. The use of EPS underneath shallow foundation do not show the correlation with the seismic response of structure if there is no interface element constructed. Variation of EPS size used were contributed to the acceleration and displacement of structure with shallow foundation. As the larger size of EPS applied, the larger reduction of seismic responses will be obtained.

**Keywords:** expanded polystyrene (EPS), interface element, numerical simulation

Being ultra lightweight with a density that is approximately 1/100 th of sand (Lin, et. al., 2010), expanded polystyrene provides a replacement for weak soils preventing settlement; a water proof material allowing for placement below the water table; and potential lower design costs and efficiency in installation as well as provides additional economic advantages for planned construction projects.

2D finite element models including beam elements and plane strain elements were constructed. This study focuses on the variation of EPS size applied to the structure and the interface element that is conducted to establish the real behavior of model. Thus the aim of this research

*Indra Waluyohadi was Student of Double Degree Master Program at National Central University and Brawijaya University. E-mail: indrawaluyohadi@gmail.com; Huei-Tsyr Chen is Professor at Departement of Civil Engineering, National Central University Jhongda Rd. 300 Jhongli City Taoyuan County, Taiwan; Achfas Zacoeb is Associate Professor at Departement of Civil Engineering, Brawijaya University JL. MT. Haryono 167 Malang, Indonesia.*

is to investigate the seismic response of structure numerically due to application of EPS applied beneath the shallow foundation using D7S2 finite element program.

Expanded polystyrene (EPS) is a closed-cell, lightweight and rigid plastic foam. It is manufactured by one of two basic processes, extrusion or steam molding. The extrusion process was introduced into the United States in 1944 and is currently used to produce either rigid board for building insulation, flotation, or as thin sheets of foam which are subsequently thermoformed into desired shapes. Generally, applications of EPS are effective for compressible geofoam material. A comprehensive treatment of geofoam material, covering their behavior, applications and design parameter has been reported by EPS Development Organization (EDO, 1992) and Horvath (1995). The widespread popularity of this kind of material is due to its several outstanding characteristics such as lightweight, compressible, water resistant and ease of use.

EPS geofoam density can be considered the main index in most of its properties. Compression strength, shear strength, tension strength, flexural strength, stiffness, creep behavior and other mechanical properties depend on the density. EPS densities for practical civil applications range between 0.1 and 0.30 kN/m$^3$. Elragi, et. al. (2000) did uniaxial test of EPS, thus Figure 1 shows the uniaxial compression stress strain curve of EPS geofoam for two different densities. The two densities shown are considered the extreme values for most engineering applications done so far.

Duskov, (1990) reported that the back calculated modulus of elasticity of EPS geofoam were found to be between 13 MPa and 34 MPa under pulse force. These values were observed to be much higher than the value of the modulus of elasticity (5 MPa) obtained under the semi static loading.

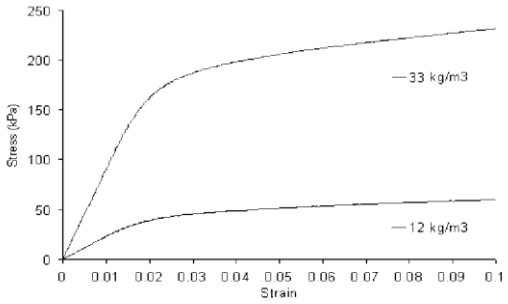


**Figure 1. EPS Uniaxial Compression Stress Strain Curves (Elragi, et. al., 2000)**

Poisson's ratio is an index of the lateral pressure of EPS geofoam on adjacent structural elements, in contact, for a certain applied vertical load on the EPS geofoam mass. Value range between 0.05 and 0.50 are found in the literature for EPS geofoam as shown in Table 1.

**Table 1. Poisson's Ratio of EPS Types**

| Reference | Poisson's Ratio |
|---|---|
| Yamanaka, et. al. (1991) | 0.075 |
| Negussey and Sun (1996) | 0.09 and 0.33 |
| Ooe, et. al (1996) | 0.08 |
| Sanders (1996) | 0.05 up to 0.20 |
| Momoi and Kokusyo (1996) | 0.50 |
| Duskov, et. al. (1998) | 0.10 |
| Geotech (1999) | 0.05 |

Sheeley (2000) did a comprehensive study of geofoam interface shear behavior for small and large samples. Normal stresses in the range of practical interest were used and different interfaces were investigated. Geofoam to geofoam interface shearing developed peak and residual strengths are shown in Figure 2.

Alzawi, A. (2011) developed comprehensive experimental and numerical investigations on the use of in-filled geofoam trench barriers to scatter machine

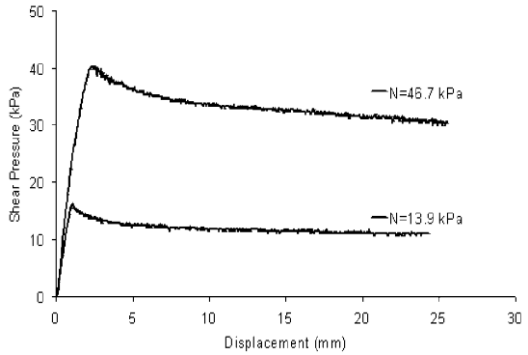


**Figure 2. EPS Interface Friction (Sheeley, 2000)**

foundations vibration. Experimental results confirmed that in-filled geofoam trench barriers can effectively reduce the transmitted vibrations and its protective effectiveness is comparable to the open trench barrier. The key parameters that influence the barrier performance are its depth and proximity to the source of disturbance, and the shear wave velocity of soil medium. The soil density, Poisson's ratio, and material damping have some influence but are less significant. Deeper trenches are required at greater distances from the source of disturbance to achieve the same level of performance. In-filled geofoam trench barrier performs more effectively in stiff soils (i.e. with relatively high vs values) than in soft soils (i.e. with low vs values). Accordingly, the soil shear wave velocity should be considered as the main soil characteristic when designing in-filled geofoam trench barriers.

Murillo, et. al. (2009) conducted the centrifuge model to examine the efficiency of EPS barriers in the reduction of traffic vibrations according to barrier width, depth and relative position in relation to the vibration source. The schematic configuration of the test is shown in Figure 3. According to the frequency ranges of vibrations due to traffic and to scaling factors for the frequency, the vibration frequencies on the models are within the range 150–2000 Hz. Efficiency of the isolation system depends on the barrier depth. When barrier depth increases, the ratio of amplitude with a barrier to the amplitude without isolation system decreases.

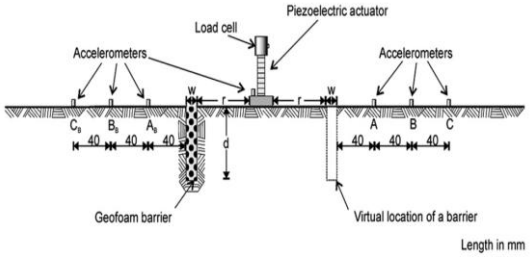


**Figure 3. Schematic Configuration of the Test (Murillo, et. al., 2009)**

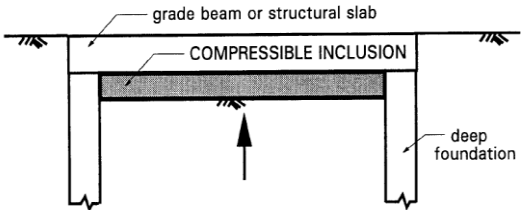


**Figure 4. Application of Compressible Inclusion Beneath Grade Beam or Structural Slab (Horvath, 1997)**

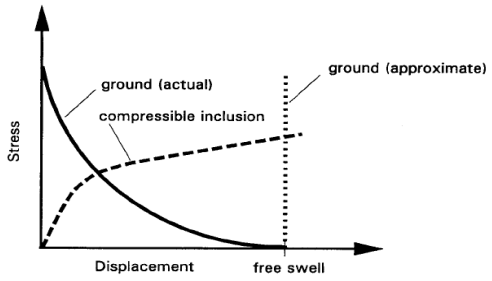


**Figure 5. Analytical Model for Expansive Ground Application Beneath Foundation Elements (Horvath, 1997)**

Horvath (1997) analyze the application, a shown in Figure 4, again involves matching the stress-displacement characteristics of the ground surface and compressible inclusion. This is illustrated conceptually in Figure 5 for the ground surface, refer to the solid curve labeled ground (actually). Rather, a site-specific stress-displacement curve for the ground is constructed, based on laboratory tests and analysis. Note that in this type of problem, only the ground is generally

considered, as compared to both lateral swell and shrinkage for applications involving earth-retaining structures.

This study focuses on the variation of EPS size applied to the structure and the interface element is also conducted to establish the real behavior of model. Thus the aim of this research to investigate the seismic response of structure numerically due to application of EPS applied beneath the shallow foundation using D7S2 finite element program.

## METHOD

Many types of interface elements have been proposed to model the interface behavior of discontinuity of two different materials. In this study the interface element proposed by Goodman, et. al. (1968) is employed to model the behavior of the interface between the two different materials. Figure 6 describes the configuration of this type of interface element. It consists of two faces labeled

$$\{\varepsilon\} = \begin{Bmatrix} U_o \\ V_o \\ W \end{Bmatrix} = \begin{Bmatrix} \frac{U_C + U_D}{2} - \frac{U_A + U_B}{2} \\ \frac{V_C + V_D}{2} - \frac{V_A + V_B}{2} \\ V_C + V_D - V_A + V_B \end{Bmatrix}$$

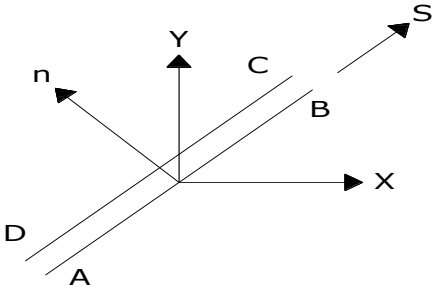


**Figure 6. Interface Element**

as A-B and C-D. The relative displacement between these two faces determines the state of the interface. Three possibilities are slippage, separation and rotation about the center of the element. Such relative displacements are computed using the spring constants $K_S$ parallel to the interface and spring constant $K_n$ normal to the interface and applied force. The strain-displacement relationship for this element is the normal and shear stresses on the joint interface are considered to be total normal and shear forces per unit area. For plane strain case, the thickness of the joint element is unity.

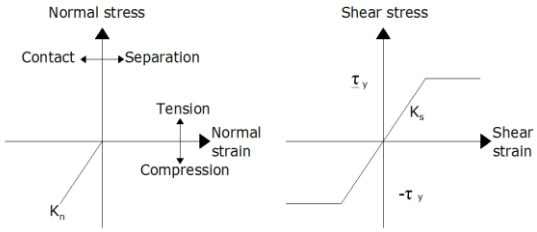


**Figure 7. Constitutive Relation for Joint Element: (a) Normal Direction and (b) Tangential Direction**

The joint element stiffness matrix obtained is for the local coordinate system (n,s). In the analysis, one has to be transformed this stiffness matrix to the global coordinate system (x,y). The constitutive relation for the interface element is shown in Figure 7. Figure 7a shows that when separation occurs, the force are not transmitted while in Figure 7b the shear behavior is assumed to follow the elasto-perfectly plastic behavior, and the yield shear is computed using the Mohr-Coulomb failure criterion.

In this study the soil non-linearity is assumed to follow the Mohr-Coulomb criterion. Referring to Figure 8, the Mohr-Coulomb failure can be written as where $\tau_y$ is the yielding shear stress, $\sigma_1$ is the maximum principal stress, $\sigma_3$ is the minimum principal stress, C is the cohesion and $\phi$ is the internal angle of friction. Depending on the values of $\sigma_m$, two types of failure exist: shear failure for $\sigma_m \leq C\cot\phi$ and tensile failure $\sigma_m > C\cot\phi$. Since in the analysis the incremental solution procedure is used,

which treats the system as linear during each load increment, the computed stress may not fall on the failure line exactly and correction is needed.

$$\tau_y = C\cos\phi - \sigma_m \sin\phi$$

$$\sigma_m = \frac{\sigma_1 + \sigma_3}{2}$$

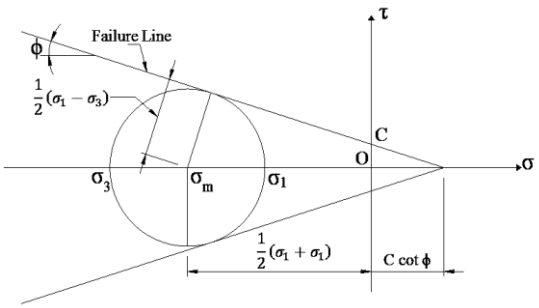


**Figure 8. Mohr-Coulomb Failure Criterion**

The problem investigated in this study involves the non-linear behavior of soil and the non-linear interface condition and is a strongly non-linear problem and the iterative process is adopted. In the solution of equation of motion the preditor-corrector scheme for Newmark method is used and the iterative solution is performed using the load-transfer approach which summarized as follows: (1) assume the soil-structure system as a linear elastic system and obtain the nodal displacements at time $t_i$ by solving the equation of motion; (2) calculate the stresses in each element from the nodal displacements; (3) estimate the maximum shear stress for each element and compare this calculated maximum shear stress with the yield stress obtained from the Mohr-Coulomb failure criterion. Also check if no separation or sliding occurs then go to the next time step $t_{i+1}$, and repeat (1) – (3) otherwise, the solution procedure goes to step (4); and (4) in this step, all unbalanced stresses are computed and converted to the quasi-external forces which are then added to the external forces, and perform the analysis by returning to step (1). This approach requires inverting the stiffness matrix only at the first time step and the subsequent time steps the inversion is avoided which leads to considerable saving of computational time.

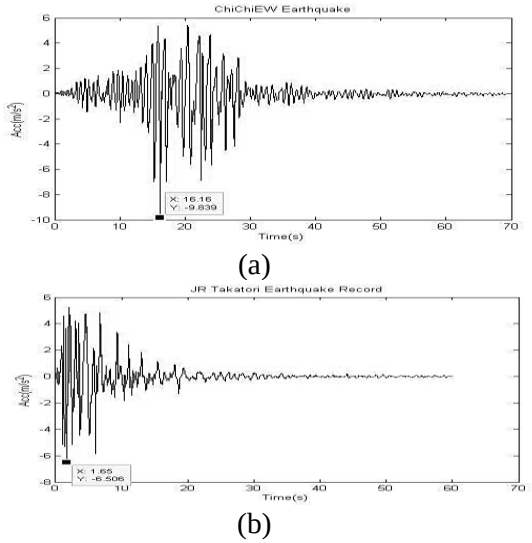


**Figure 9. Input Motion (a) Chichi Earthquake 1999; (b) JR Takatori Earthquake**

Two acceleration time-history were used as input motion. The first is during 1999 Chichi earthquake measured at the Sun Moon Lake station and the second is 1995 Kobe earthquake which observed at JR Takatori station. Figure 9 shows the time history of 1990 Chichi earthquake and JR Takatori earthquake record. It can be seen that the characteristics are different; it is possible to see the effect of earthquakes on the seismic responses of structure with an EPS.

Verification and validation study was also conducted as the preliminary study of this research. In this study the result of shaking table test of model of EPS done by Lee (2012) used to validate and verify the model constructed by using D7S2. The model should be good enough, which depends on the goal of the model. The shaking table test was performed at the National Central University (NCU), Taiwan. The shaking table has 3.00 m long x 2.00 m wide of table size,

maximum load capacity 6 tons, maximum displacement ±350.00 mm and ±200.00 mm in x and y-axis respectively. Maximum velocity is ±1.20 m/s in x-axis and y-axis, maximum acceleration in x-axis of 9.90 m/s$^2$ and 8.80 m/s$^2$ for y-axis. Frequency range of shaking table has 0.01 Hz to 50 Hz and used hydraulic actuator as drive device. Control pattern of shaking table are used for displacement, acceleration and input signal control, maximum sampling rate of data acquisition is 10.00 kHz.

Model has three layer of 1.30 m wide x 0.60 m thick of EPS with trapezoidal cross section. Two layers of 1.30 m wide x 2.00 cm thick of steel plate were placed between the EPS layer. Concrete block with dimension 2.96 m long x 1.30 m wide x 0.40 m thick approximately were rest on first layer of EPS. The model sit on the 2.00 cm thickness of inclined plate with inclined 2.76 m horizontal x 1.86 m vertical approximately, the model configuration can be seen in Figure 10. The inclined plate supported by four column made by H 200 x 200 beam column.

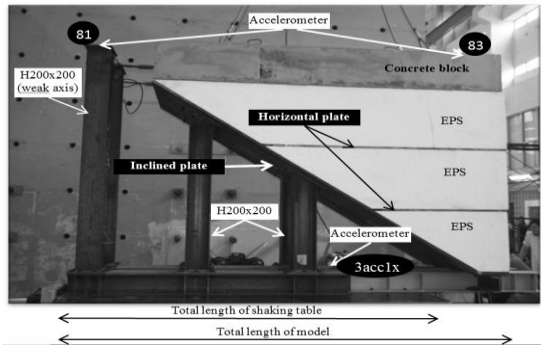


**Figure 10. Model Configuration of Shaking Table Test (Lee, 2012)**

D7S2 program was used to analyze the constructed model based on the experimental model. Two dimensional finite element plane strain model are applied with dynamic analysis. All the steel structure supported the EPS and concrete were model as beam element, except inclined plate and horizontal plates were modeled as plane strain element. EPS, concrete and plates between EPS layer also construct as plane strain element can be seen in Figure 11. The parametric values of all materials described in Table 2, and the scale factor of model between numerical simulation and the experiment is 1.

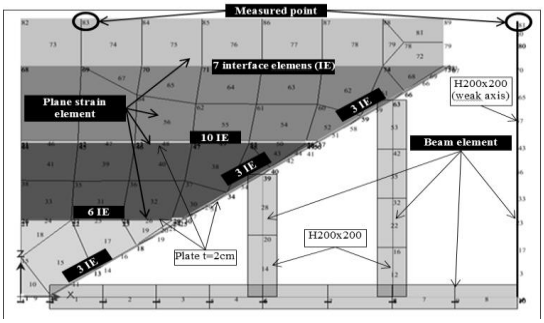


**Figure 11. Numerical Model**

Input motion of shaking table test which is Sun Moon Lake input record during the 1999 Taiwan Chichi earthquake is used, and then acceleration measured on the shaking table is used for the input motion of numerical simulation. The input motion has 32.50 second time duration and peak ground acceleration of 22.42 m/s$^2$ at 11.34 s. It has predominant frequency of 11.66 Hz.

Figure 12 shows the FFT and transfer function for cases with interface element. The natural frequency of system is 4.88 Hz, it has the same value with the experimental result. Thus, good agreement is observed between the numerical simulation and experiment.

Figure 13 shows the comparison of time history between the experiment (acc81-EXP) and the numerical simulation (acc81-NIE and acc81-IE). As can be seen, the response from numerical simulation slightly lower than those in experiment. The maximum response from the numerical simulation is around -73.50 m/s$^2$, and -78.93 m/s$^2$ from experimental result. Also small different for response when motion start to amplifies. However,

the trend in general is similar between the numerical simulation and the experiment, good agreement is observed.

## RESULTS

This part presents the effect of EPS on the seismic responses of frame rested on the shallow foundation. The numerical analysis is performed by using D7S2 finite element program. A series of parametric study is conducted including the interface element and the variations of size of EPS.

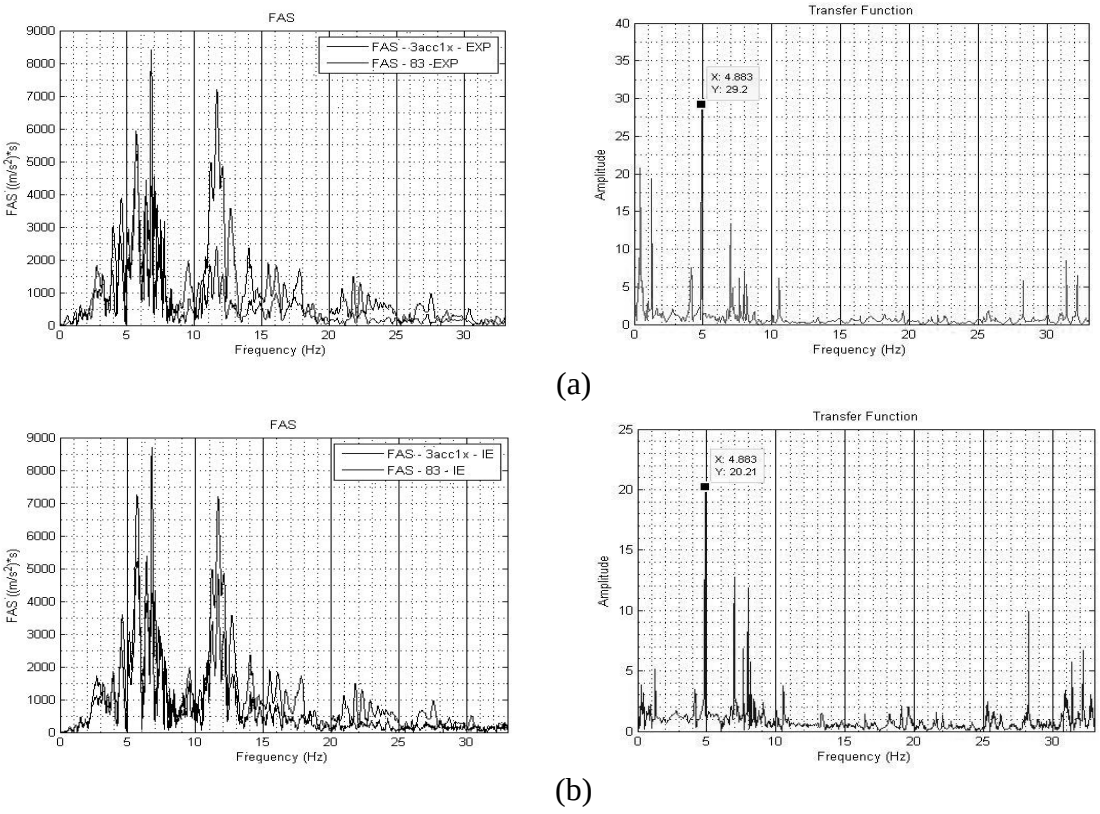


**Figure 12. FFT and Transfer Function for (a) Experimental Result (acc83-EXP); (b) Case with Interface Element (acc83-IE)**

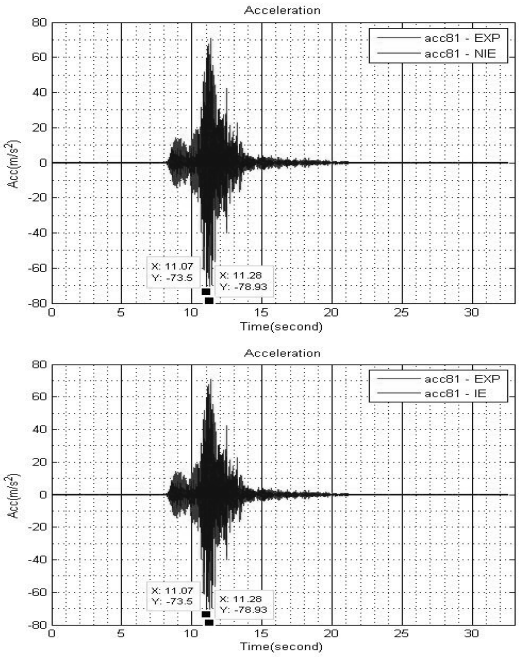


**Figure 13. Comparison of Time History at Point 81 of Experimental Result and Numerical Result**

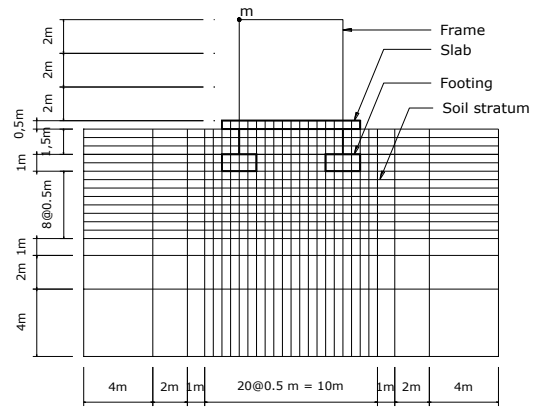


**Figure 14. Model without EPS and Interface Element for Hard Soil Stratum and Soft Soil Stratum**

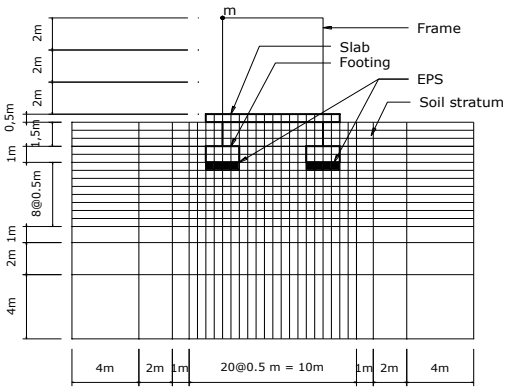


**Figure 15. Model with 2.00 m x 0.50 m EPS**

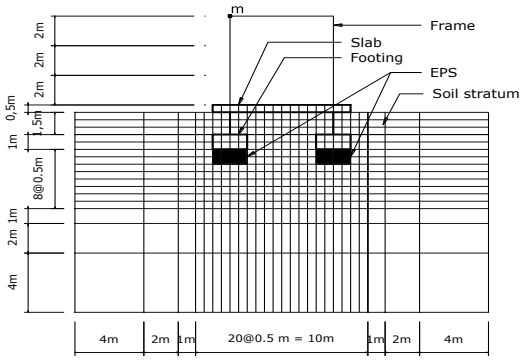


**Figure 16. Model with 2.00 m x 1.00 m EPS**

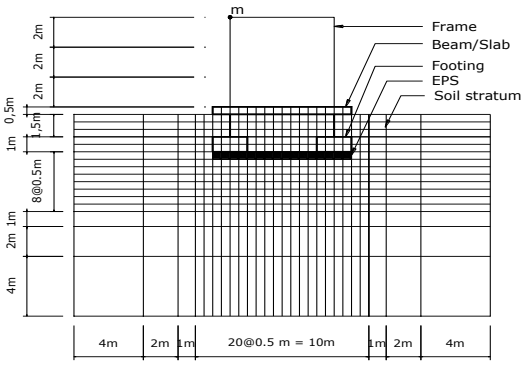


**Figure 17. Model with 8.00 m x 0.50 m**

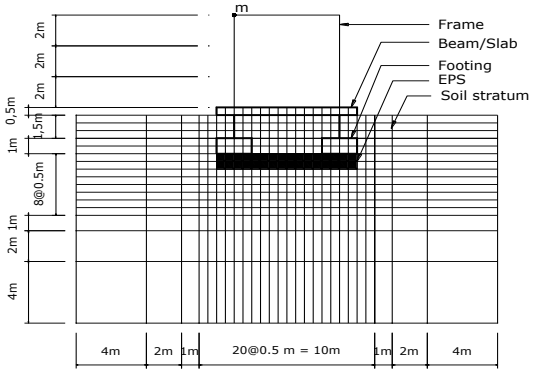


**Figure 18. Model with 8.00 m x 0.50 m**

out EPS and interface element are constructed. The first model is hard soil stratum denoted as HS model, and the second model is model with soft soil stratum denoted as SS. Figure 14 shows the

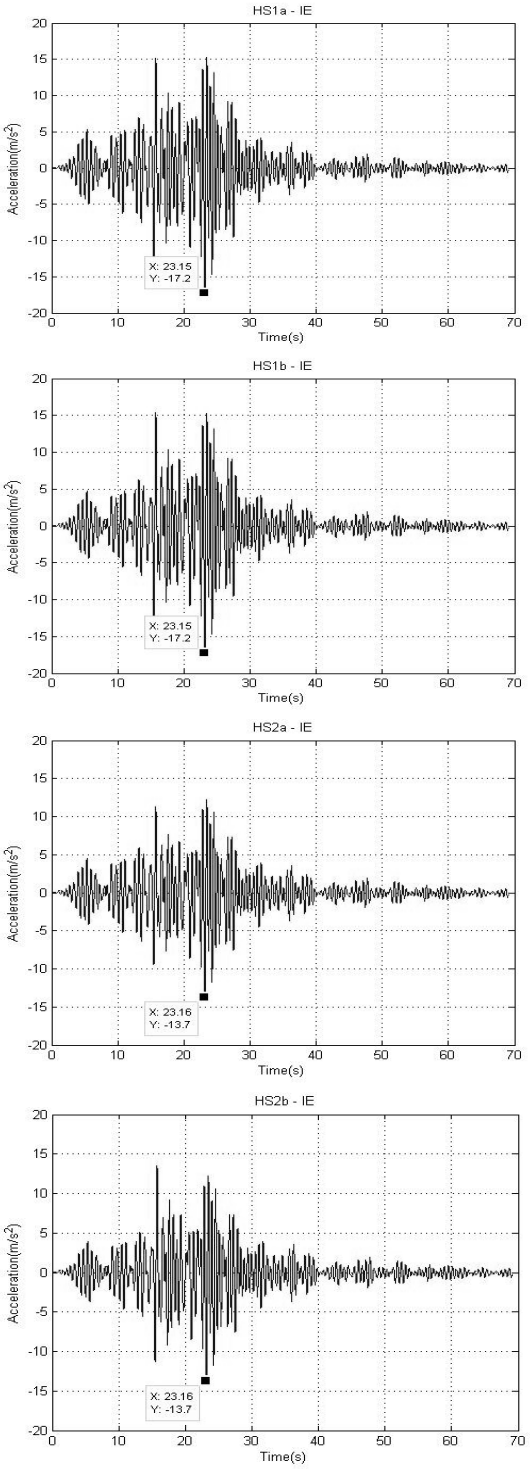


**Figure 19. Acceleration of Hard Soil Stratum Models for Chichi Earthquake Input Motion**

finite element model for both cases. The model consists of plane strain element and beam element, in which has dimensions of 24 m x 13.5 m (width x depth) of soil stratum and 6 m x 6 m (width x high) of concrete frame. Column of foundation and frame modeled as beam element then soil stratum, footing, and slab modeled as plane strain element. Shallow foundations with 2.50 m depth were conducted, including 1 m of footing.

The followed cases were several models of EPS beneath the footing, which are 2.00 m and 8.00 m width of 0.50 m and 1.00 m thickness. These configurations of EPS layer were conducted for both hard soil stratum and soft soil stratum cases shown in Figure 15 – 18. Thus table 2 shows the parameter value in this study.

Figure 19 shows the results of hard soil stratum models with interface element by Chichi earthquake input motion. The maximum acceleration of HS1a–IE, HS1b–IE, HS2a–IE and HS2b–IE are -17.20, -17.20, -13.70 and -13.70 m/s$^2$ respectively.

Shown in Figure 20 are the acceleration of soft soil stratum models with interface element. Maximum aceleration reduced from -24.60 m/s$^2$ to -18.50 m/s$^2$ for SS1a-IE and SS1b-IE model, and -14.70 m/s$^2$ for SS2a-IE then 14.90 m/s$^2$ of SS2b-IE model.

Figure 20 also shows the variation thickness of EPS did not affect the maximum acceleration, except SS2b-IE has 14.90 m/s$^2$ at 15.73 s.

Displacement response of point m of hard soil stratum models for Chichi earthquake input motion can be seen in Figure 21. The maximum displacement of model HS1a-IE, HS1b-IE, HS2a-IE and HS2b-IE are 0.00015, 0.15, 0.12 and 0.12 m respectively. The displacements

**Table 2. Parametric Values of Model**

| No. | Material Parameters | Plane Strain Element | | | | | Beam Element | | Interface Element |
|---|---|---|---|---|---|---|---|---|---|
| | | Hard Soil | Soft Soil | EPS | Slab | Footing | Frame | Column Foundation | |
| 1 | Shear Wave Velocity – Vs (m/s) | 500 | 300 | 310.63991 | 2069.901 | 2069.901 | | | |
| 2 | Poisson's Ratio - v | 0.3 | 0.4 | 0.075 | 0.167 | 0.167 | | | |
| 3 | Rayleigh's damping - α | 0 | 0 | 0 | 0 | 0 | | | |
| 4 | Rayleigh's damping - β | 0.009 | 0.0090123 | 0.009 | 0.009 | 0.009 | 0.009 | 0.009 | |
| 5 | Mass Density – t/m$^3$ | 1.9 | 1.8 | 0.02041 | 2.5 | 2.5 | 2.5 | 2.5 | |
| 6 | Cohesion – N/m$^2$ | 145040 | 100000 | 100000 | 100000 | 100000 | | | |
| 7 | Angle of friction - φ | 12 | 12 | 36.88 | 30 | 30 | | | |
| 8 | Young's modulus (kN/m$^2$) | 0 | 0 | 0 | 0 | 0 | 2.5E+07 | 2.5E+07 | |
| 9 | Moment of inertia – m$^4$ | 0 | 0 | 0 | 0 | 0 | 0.000675 | 0.000675 | |
| 10 | Normal stifness - Kn | | | | | | | | 1.0E+18 |
| 11 | Normal stifness - Ks | | | | | | | | 400000 |
| 12 | Cohesion before sliding (kN/m$^2$) | | | | | | | | 4 |
| 13 | Friction angle before sliding - φ | | | | | | | | 30 |
| 14 | Cohesion after sliding (kN/m$^2$) | | | | | | | | 4 |
| 15 | Friction angle after sliding - φ | | | | | | | | 30 |

reach maximum at the same time duration, which is about 23.16 seconds.

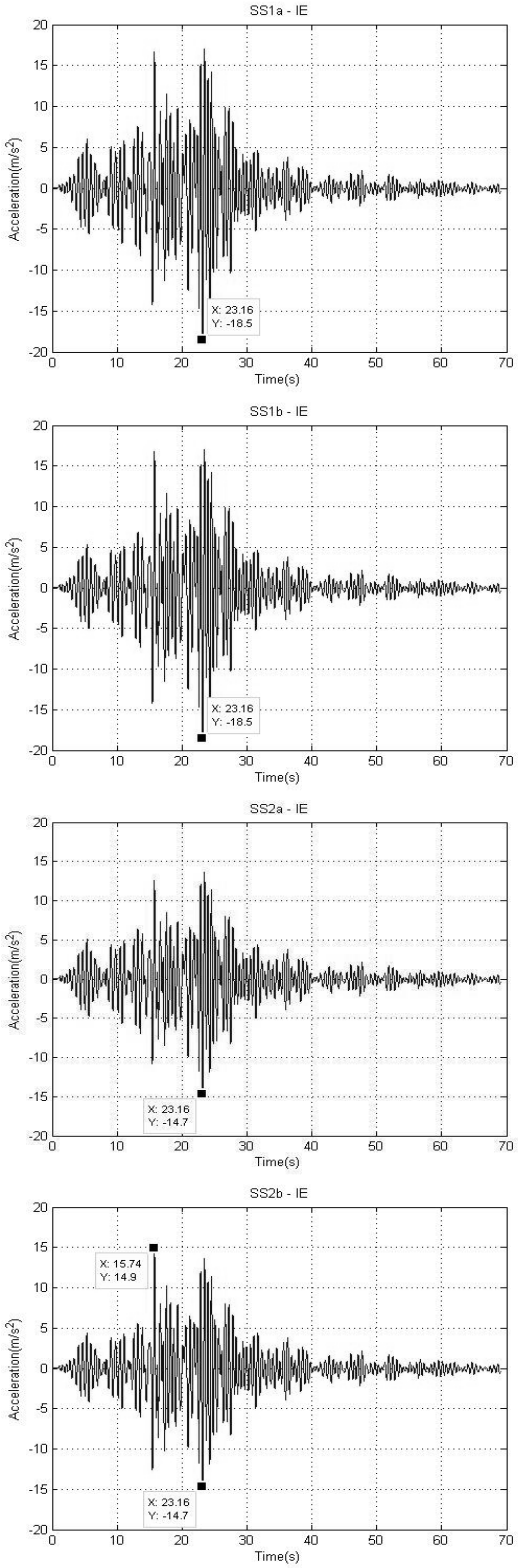


**Figure 20. Acceleration of Soft Soil Stratum Models for Chichi Earthquake Input Motion**

Figure 22 shows the displacement of point m of soft soil stratum models for Chichi earthquake input motion. The maximum displacement were 0.16 m of cases with 0.50 m thickness of EPS

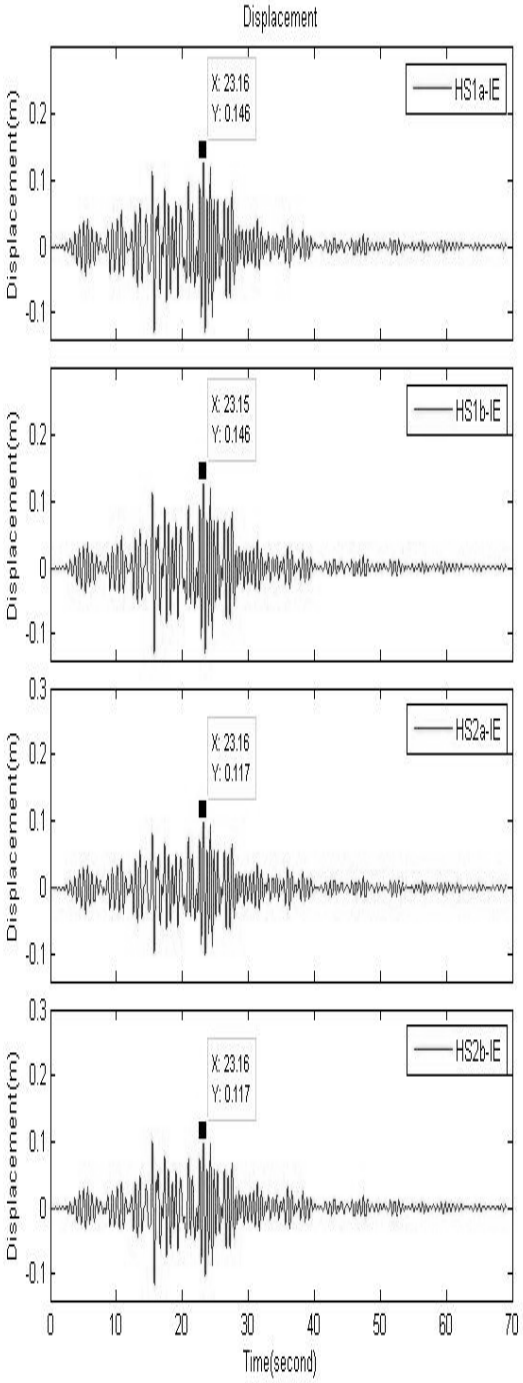


**Figure 21. Displacement of Point m of Hard Soil Stratum Models for Chichi Earthquake Input Motion**

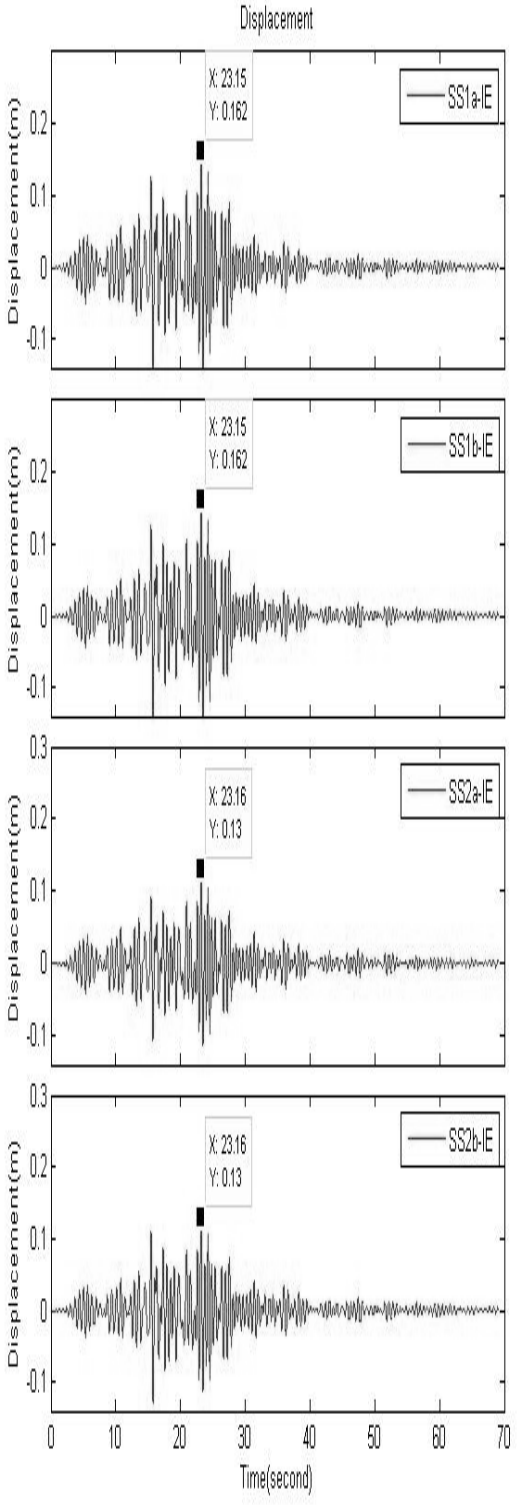


**Figure 22. Displacement of Point m of Soft Soil Stratum Models for Chichi Earthquake Input Motion**

(model SS1a-IE and SS1b-IE), and 0.13 m of cases with EPS thickness 1.00 m (model SS2a-IE and SS2b-IE).

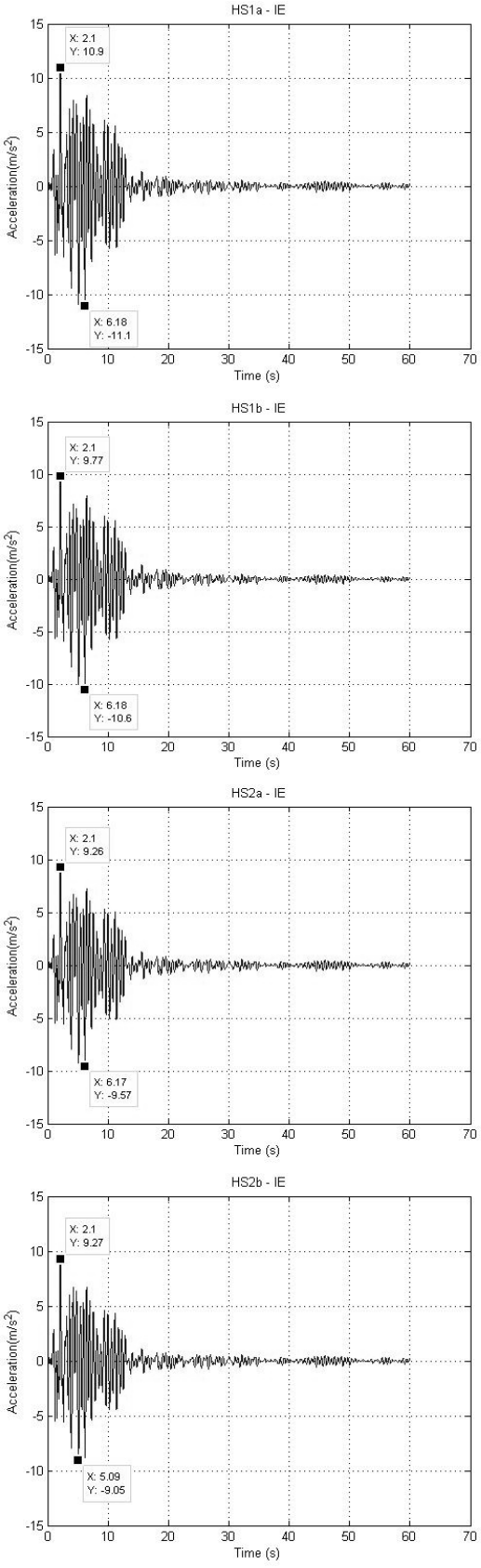


**Figure 23. Acceleration of Hard Soil Stratum Models for JR Takatori Earthquake Record Input Motion**

Figure 23 depicts the acceleration of hard soil stratum models for JR Takatori Earthquake record input motion. The maximum accelerations were occurred at 6.19 seconds for all models except HS2b-IE model was occurred at 2.10 seconds. The largest acceleration was HS1a-IE model, which is -11.10 m/s$^2$. The maxi-

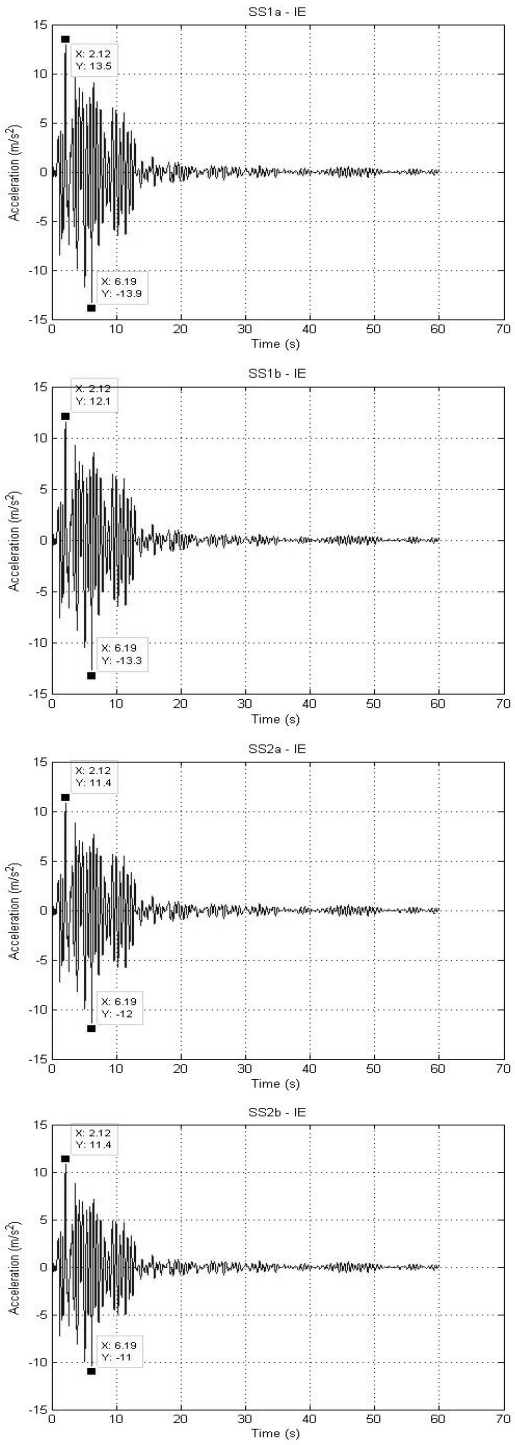


**Figure 24. Acceleration of Soft Soil Stratum Models for JR Takatori Earthquake Record Input Motion**

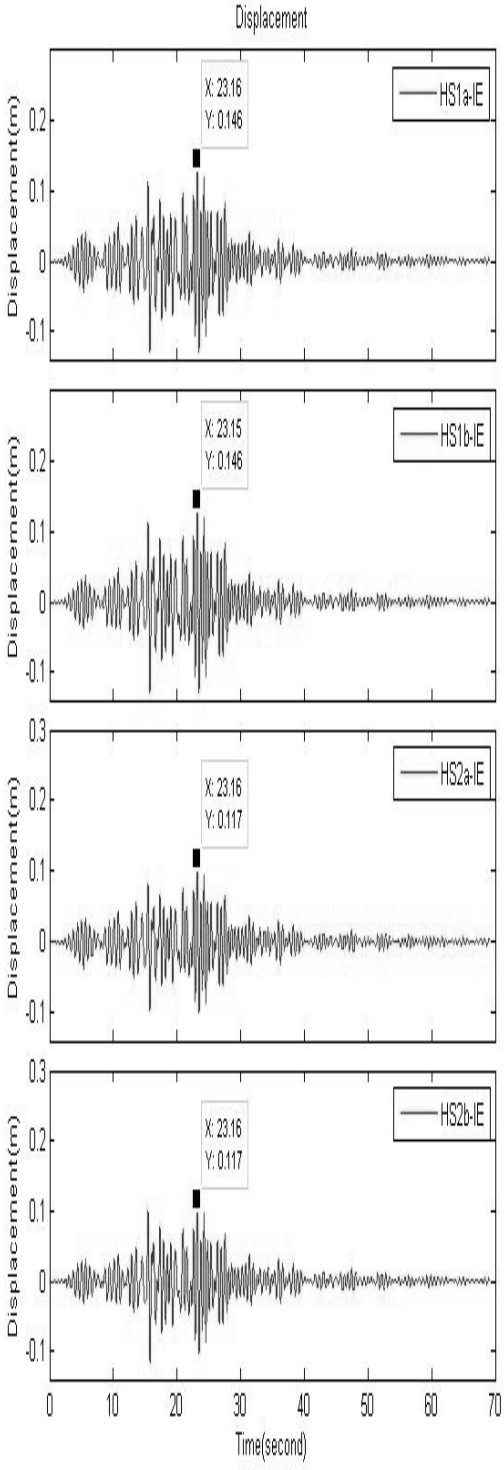


**Figure 25. Displacement of Point m of Hard Soil Stratum Models for JR Takatori Earthquake Record Input motion**

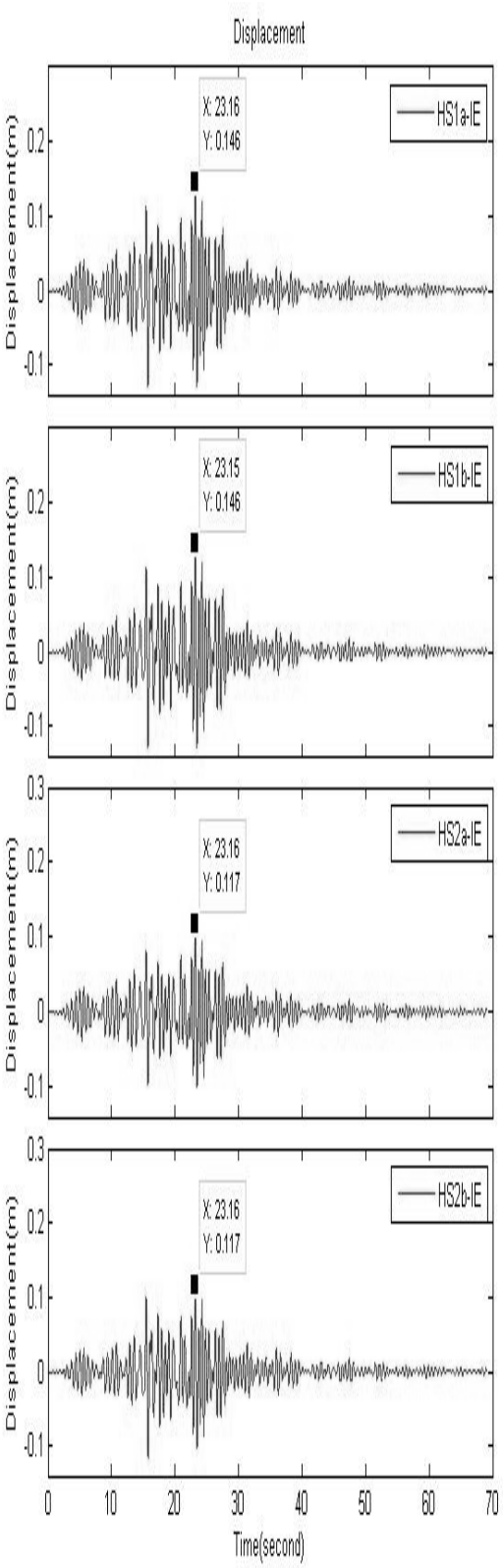


**Figure 26. Displacement of Point m of Soft Soil Stratum Models for JR Takatori Earthquake Record Input Motion**

mum acceleration of HS1b-IE, HS2a-IE and HS2b-IE model are -10.6, -9.57 and 9.27 m/s$^2$ respectively.

Time history at point m of acceleration response of soft soil stratum models for JR Takatori earthquake record input motion can be seen in Figure 24. The response of SS1a-IE, SS1b-IE and SS2a-IE were amplified around 6.19 seconds, with the maximum acceleration -13.90,-13.30, -12.00 m/s$^2$ respectively.

The smallest acceleration was SS2b-IE model, which around 11.40 m/s$^2$ and amplified at 2.10 s.

Displacement of point m of hard soil stratum models for JR Takatori earthquake record input motion can be seen in Figure 25. The maximum displacement of HS1a-IE, HS1b-IE, HS2a-IE and HS2b-IE model are 0.10, 0.09, 0.08, and 0.08 m respectively.

Figure 26 shows the time history of displacement of point m on Soft soil stratum models under JR Takatori Earthquake Record Input Motion. The similar observation obtained for displacement on hard soil models, the largest displacement was model with smallest size of EPS. The maximum displacement of SS1a-IE, SS1b-IE, SS2a-IE and SS2b-IE are 0.11, 0 010, 0.90, and 0.90 m respectively.

## DISCUSSIONS

The results of hard soil stratum models with interface element by Chichi earthquake input motion. Shows the response between HS1a–IE and HS1b–IE cases and also between HS2a – IE and HS2b–IE cases seems the same. Besides, the acceleration of soft soil stratum models with interface element compared to cases without interface element shows the effect of development of interface element is significant. As same as hard soil stratum cases, case with interface

element gives the smaller acceleration response. This phenomenon is agreed with the characteristic of Goodman interface element when the assumption of the zero thickness of interface element applied. This research also considered to the passive isolation system. Referris to the Woods (1968), the EPS are applied beneath the shallow foundation, where the vibratory amplitude must be reduced is defined as passive isolation systems.

The variation thickness of EPS did not affect the maximum acceleration, except SS2b-IE has 14.90 m/s$^2$ at 15.73 s. It may be model with thicker EPS on soft soil stratum easier to amplified than model on hard soil stratum.

Displacement response of point m of hard soil stratum models for Chichi earthquake input motion can be seen in Figure 21. It can be observed that development of interface element not only affect the maximum displacement of model with variation of width of EPS, but also model with variation of thickness of EPS. Besides, the displacement of point m of soft soil stratum models for Chichi earthquake input motion, the similar effects as hard soil stratum cases were obtained; the variation of thickness of does not affect the maximum displacement. There is no literature compared to this cases in the point of displacement, as far as the EPS applied beneath to the structure.

The largest acceleration of hard soil stratum models for JR Takatori Earthquake record input motion was model with smallest size of EPS applied beneath shallow foundation. Besides, the variation of EPS sizes were also induced the acceleration, which increased the thickness and width of EPS give the smaller acceleration. This result has same characteristic with the experimental results done by Murillo, et al. (2009). The efficiency of the isolation system depends on the EPS sizes. When the EPS sizes increases, the ratio of amplitude with EPS to the amplitude without EPS isolation system decreases.

Behavior of EPS with interface element on soft soil stratum model showed similar to those for the same variation of EPS on hard soil model. Since EPS sizes applied beneath the shallow foundation become larger, thus maximum displacement of structure decreases. Developments of interface element made the possibility of the shallow foundation slide, and reduce the displacement of structure. The similar observation obtained for displacement on hard soil models, the largest displacement was model with smallest size of EPS.

The interface strength between geofoam and geomembrane surfaces was low. Substitution of a concrete load distribution slab with a geomembrane may therefore result in much weaker interface. This result is agree with Sheeley (2000). The key parameters that influence the barrier performance are its depth and proximity to the source of disturbance, and the shear wave velocity of soil medium. The soil density, Poisson's ratio, and material damping have some influence but are less significant.

The magnitude of stress from the heaving ground depends on the stress-displacement properties of the ground and stiffness of the compressible inclusion. As results obtained by Horvath (1997), the compressible inclusion must be sufficiently stiff so that it does not compress excessively during foundation construction. For given compressible inclusion thickness (i.e. stiffness), the ac-

tual stress on the foundation from the heaving ground will be somewhat less anticipated.

## CONCLUSIONS AND RECOMMENDATIONS

From the observation and the analysis of the simulation results, several conclusions are listed as follows: (1) the use of EPS for reducing the acceleration and displacement is effective for all cases subjected to Chichi earthquake and JR Takatori earthquake record input motion both models with hard soil stratum and soil stratum; (2) for models on hard soil stratum and soft soil stratum subjected to the Chichi earthquake motion, maximum acceleration and maximum displacement only affected by variations of width of EPS; (3) for model subjected to the JR Takatori earthquake record input motion, the variation of thickness and width of EPS were contributed to the reduction of maximum acceleration and maximum displacement; and (4) generally, the reduction in maximum acceleration and displacement is due to the fact of development of interface element. Variation of EPS size used were contributed to the acceleration and displacement of structure with shallow foundation. As the larger size of EPS applied, the larger reduction of seismic responses will be obtained.

Earthquake with different characteristic gives different seismic responses of structure. This implies the importance of using the motion recorded at the site construction to evaluate the effectiveness of EPS. Further investigation of EPS applied on the liquefiable soil stratum to deepen understanding its effect on the seismic response. The use of various configurations of EPS should be carried out to be able to access the effectiveness of each configuration in reducing the seismic response. The properties of EPS must be defined as well as the objective of experiment or research and considering the factory of EPS.

## REFFERENCES

Alzawi, A. 2011. *Vibration Isolation using In-Filled Geofoam Trench Barriers.* PhD Thesis, University of Western Ontario.

Duškov, M. 1990. *Falling Weight Deflection Measurements on Asphalt Test Pavements with EPS at the Bunesanstalt fur Strassenwesen.* Study, Faculty of Civil Engineering, Delft University of Technology, Delft, The Netherlands.

Elragi, A., Negussey, D., & Kyanka, G. 2000. *Sample Size Effect on the Behavior of EPS Geofoam*. Proceedings of the Soft Ground Technology Conference, The Netherlands.

EPS Development Organization (EDO). 1992. *Expanded Polystyrene Construction Method.* Riko Tosho Publishers, Tokyo, Japan.

Gooodman, R.E., Taylor, R.L., & Brekke, T.L. 1968. A Model for the Mechanics of Jointed Rock. *Journal of the Soil Mechanics and Foundations Division* ASCE, 94(3): 637–659.

Horvath, J.S. 1995. *Geofoam Geosynthetic*. New York, USA: Horvath Engineering, P.C., Scarsdale.

Horvath, J.S. 1997. The Compressible Inclusion Function of EPS Geofoam. *Geotextiles and Geomembranes* 15: 77-120.

Lee, T.Y. 2012. *Data of Shaking Table Test of EPS Model.* NCU, Taiwan.

Lin, P., Abrahamson, N., Walling, M., Lee, C.T., Chiou, B., & Cheng, C.

2010. *Repeatable Path Effects on the Standard Deviation for Empirical Ground Motion Modelsl.* Berkeley: University of California.

Murillo, C., Thorel, L., & Caicedo, B. 2009. Ground Vibration Isolation with Geofoam Barriers: Centrifuge Modeling. *Geotextiles and Geomembranes*, 27: 423–434.

Sheeley, M. 2000. *Slope Stabilization Utilizing Geofoam.* Master‟s Thesis, Syracuse University, Syracuse, NY, USA.